Available online at www.sciencedirect.com
SCIENCE DIRECT®
Journal of Photochemistry and Photobiology A: Chemistry 168 (2004) 31–38
Journal of Photochemistry and Photobiology A:Chemistry
www.elsevier.com/locate/jphotochem

Spectroscopic and dynamic studies of the photolysis reaction of acetone by 193 nm excimer laser

Y. Badr [a], S. Abd El-wanees [b], M.A. Mahmoud [b,*]

[a] National Institute of Laser Enhanced Science, Cairo University, Cairo, Egypt
[b] Chemistry Department, Faculty of Science, Zagazig University, Zagazig, Egypt

Received 31 March 2004; accepted 13 May 2004
Available online 2 July 2004

Abstract

The high-resolution time resolved Fourier transformed IR spectroscopy is used here to measure the emitted spectra of the CO fragment resulting from the photolysis of acetone by 193 nm excimer laser. A high-resolution IR spectra in the range of 1950–2250 cm^{-1}, is assigned to be CO ro-vibrational transition. The vibrational population of the first four vibrational levels were obtained by simulating of these spectra. The vibrational temperature $T_{Vib.}$ of the CO was found to be 2250 ± 70 K as given from the Boltzmann plot. Moreover, the Boltzmann distribution was found to fit the rotational degrees of freedom yielding a characteristic temperature $T_{Rot.}$ of the CO of about 2250 K in the case of low relaxation and 1 μs time delay experiment. The prior distribution model was found to predict the vibrational and rotational energies lower than the measured values. While the impulsive model predicts higher values, the statistical adiabatic model used here was found to predict values for E_T, $E_{Vib.}$, $E_{Rot.}$ according well with the measured experimental values.

Keywords: Vibrational; Impulsive model; Boltzmann

1. Introduction

As the simplest ketone, acetone has long been used as prototype for studying of photophysics and photochemistry of this important class of carbonyl compounds. Photolysis proceeding via α-bond cleavage (Norrish I) is most studied of the photochemical processes [1].

At sufficiently high excitation energies, acetone represents a prototypical three body dissociation process involving the cleavage of two identical chemical bonds of dynamical interest is extended to which the two bond breaking steps are energetically and temporally coupled.

Recent studies on the photodissociation dynamics of acetone, showed that the sequence of events leading to the three asymptotically separated fragments is still largely unresolved. The review of Lee and Lewis [2] summarized most of the photochemical research from the pre-laser era.

Baba et al. [3] measured the yield of acetone fragment ions following multiphoton excitation by an ArF excimer laser at 193 nm, the power dependence of the acetyl ion signal ($m/e = 43$) suggested that the ion was produced as a result of absorption of the laser radiation by a relatively long-lived neutral acetyl fragment. They considered this result as an evidence of a sequential bond rupture mechanism. The initial excitation is to the A adiabatic potential energy surface which is bound along the C–C coordinate. Bond cleavage can occur by either internal conversion or intersystem crossing to the $C_s\sigma^3\sigma^*$ configuration via out-of-plane motion [4,5]. Consequently, excited state dissociation can proceed over a small barrier caused by an avoided crossing on the T_1 surface. This barrier height has been measured by Zuckermann et al. [6] who observed a pronounced decrease in the fluorescence emission at 305.8 nm. The excimer laser operating at 193 nm ArF transition is used to photodissociate acetone because the acetone absorption cross-section at 193 nm is large (2×10^{-18} cm^2) [3].

Brouard et al. [7] measured the quantum yields for the various dissociation pathways following 193 nm excitation. For acetone the dominant fragmentation is $(CH_3)_2CO \rightarrow CH_3 + CO + CH_3$, with a quantum yield of 0.96.

Excitation at 248 nm resulted in the production of CH_3 and CH_3CO. The nascent acetyl radicals from the primary dissociation contain sufficient energy to undergo spontaneous decomposition [8].

* Corresponding author.
E-mail address: mahmoudchem@yahoo.com (M.A. Mahmoud).

1010-6030/$ – see front matter © 2004 Elsevier B.V. All rights reserved.
doi:10.1016/j.jphotochem.2004.05.013

Potzinger et al. [9] photolyzed acetone at 185 nm with a low-pressure mercury arc and determined quantum yield Φ of final products to be ∼1 for CO and ∼0.95 for C_2H_6. Gandini and Hackett [10] found that the quantum yield for carbon monoxide production in the region 255–280 nm was unaffected by the addition of several hundred Torr of an inert bath gas and concluded that the direct route to carbon monoxide production was most likely. Donaldson and Leone [11] have detected the infrared emission as a function of time from the excited CH_3 and CO resulting from the 193 nm photolysis of acetone, their results strongly suggests that the three body dissociation occurs via a two step mechanism, rather than a vigorously concerted process. Woodbridge et al. [12] have been studied the photophysics and photochemistry of acetone excited to its lowest $^1(n, {}^*\pi)$ excited state at wavelengths longer than 200 nm, the primary photoproducts of acetone in this special region are CH_3 and CH_3CO, with a strong dependence on pressure, temperature and excitation wavelength. At low pressures, dissociation primary occurs from vibrationally excited levels of the strongly mixed $^1(n, {}^*\pi)$ and $^3(n, {}^*\pi)$ states. At higher pressures, there is a temperature dependent dissociation of both the vibrationally relaxed triplet and the acetyl radical to yield a second methyl radical and CO. The only temporally resolved studies on the 3S Rydberg state are those by Buzza et al. [13] who used femtosecond laser pulses at 585 nm to induce a three photon absorption to the 3S Rydberg state, followed by two photon ionization at the same wavelength to monitor the mass-resolved dynamics of the acetyl radical.

Zewail and coworkers [14] measured the lifetime of the 4S Rydberg state in acetone using femtosecond REMPI laser following two photon excitation at 307 and 280 nm. Kim and Zewail [15] also examined the dissociation of acetyl as the secondary step in several asymmetric ketones. Ultrafast deep UV mass-resolved photoionization spectroscopy has been used to investigate the photodissociation dynamics of the 3S Rydberg state of acetone. Single photon excitation at 193–195 nm is followed by single photon at 260 nm and two photons at 390 nm ionization. The signals are measured for both the acetone and acetone photoions [16].

Shibata et al. [17] measured the ion images of the acetyl radical as a function of pump-probe time delay. The time resolved FT-IR spectroscopy was used to account for the time sequences of the photolysis of acetone by 193 nm excimer laser pulses for different delay times (2, 10, 20, 30, and 50 μs) by Badr et al. [18]. In the present work the time resolved FT-IR spectroscopy are used to account for the photolysis of acetone by 193 nm excimer laser pulses. aiming to account for the possibility of resolving the IR spectra as detected by the previous work.

2. Experiment

The time-resolved Fourier transform IR has been described in detail previously [19]. Some modifications have been made for these experiments: (1) the IR source is replaced by the emission from the fragments resulting from the photodissociation by the laser; (2) the function generator in the (TR-SS) is replaced by the delay generator, which consists of a function generator (Stanford research system, Model DS 345, 30 MHz) connected to a delay unit (Stanford research system, Model DG 535). This set-up gives two signals which are delayed from each other by sub-microseconds. The delayed signal is given to the FT-IR (Bruker IFS 66V) spectrometer, while the original one is given to the external trigger of the 193 nm ArF excimer laser (Lambda Physics) via a light-emitting diode. The photolysis mixture, consisting of either acetone or acetone and helium are introduced to the photolysis chamber [20]. The ArF excimer laser pulses pass through the chamber and photolyze acetone. Time-resolved IR vibrational emissions from vibrationally excited photofragments produced by the dissociation are detected through the TR-FT-IR.

3. Results

3.1. The vibration–rotation spectrum of CO

The time resolved emission FT-IR is a high-resolution technique because it allows us to resolve the emitted spectra of the molecules over a broad wavelengths range in a relatively short period of time. Such a high-resolution spectra can be analyzed directly to obtain the ro-vibrational state populations. When a mixture of acetone and He photodissociated by 193 nm excimer laser pulses acetone undergoes dissociation to vibrationally excited CO and two CH_3 radicals. The presence of He buffer gas serves as a rotationally relax photoproducts on a short period of time.

Three experiments were done: 0.1 Torr acetone and 10 Torr He, 0.2 Torr acetone and 30 Torr He, 0.15 Torr acetone under the same conditions, laser power (4.2 MW/cm^2) and time delay 10 μs.

The emission spectra in the (1950–2250 cm^{-1}) region revels the ro-vibrational bands of CO molecule. At least three vibrational levels are populated in CO molecule. The coupling between (P and R) branches of the (vibration–rotation) spectra takes place in the experimental spectra of CO; so to resolve this spectrum we should “simulate” the experimental spectra theoretically. The simulated spectra resulted from plotting the intensity per vibrationally excited molecule versus the frequency of the individual transition. To determine the relative vibrational populations, we simply measured the areas of the peaks, dividing it by the appropriate Einstein spontaneous emission coefficient, and sum over the vibrational states. Einstein coefficients were calculated using methods and constants given in reference [21]. Only the lines that are fully resolved in all the three levels are used for such analysis. The areas of the peaks calculated after Gaussian fitting for every rotational line. The row spectra obtained are a convolution of the actual emission intensity with the

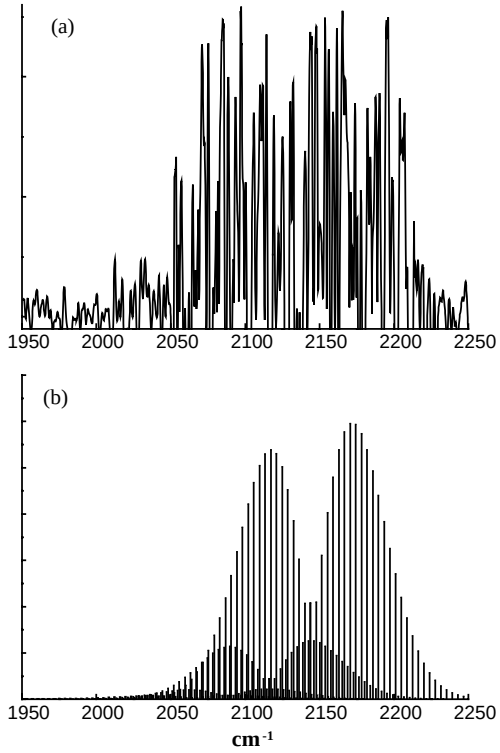

Fig. 1. A comparison of the observed and simulated spectra (upper spectra) the experimental spectrum of CO emission obtained from the photodissociation of 0.1 Torr acetone and 10 Torr He by the 193 nm excimer laser at time delay 10 μs (lower spectrum) the simulated spectrum of CO at rotation temperature 300 K.

response function of the detector, the transmission/reflection functions of all the optics, and the black body background. To correct the spectra, a very high (S/N) ratio spectrum is taken without pulsing the laser. The raw spectra are then divided by this instrumental response function to obtain a spectrum that reflects the true emission.

Fig. 1 shows the optimized spectral simulations according to our calculations. The higher spectrum (a) is the experimental rotational vibrational spectrum of CO molecule resulting from the photodissociation of 0.1 Torr acetone and 10 Torr He at time delay 10 μs after the 193 nm excimer laser with power (4.2 MW/cm^2) pulse. The lower spectrum (b) represents the rotation vibration simulated spectrum of CO. The vibrational population of the first four vibrational levels of CO molecule can be calculated from both the experimentally obtained fully resolved rotational lines and the simulated ones.

Table 1 gives the vibrational populations of the first four vibrational energy levels of CO molecule resulting from the photodissociation of the above three experiments.

3.2. The rotational temperature of CO molecule

In the presence of He in the photolysis mixture, the S/N ratio is expected to be very low (poor) consequently; it will be nearly impossible to obtain good-resolved rotational lines for each individual vibrational state. Moreover many of the bands in the spectra are overlapped, containing contributions from two or three excited vibrational levels. In addition to the first excited level ($v = 1$) whereas the rotational lines in the vibrational state (v) can be used to determine the rotational temperature using the Boltzmann's rotational plot. Since the thermal rotational distribution within a single vibrational levels is given by the Boltzmann's expression in equation:

$$I^{(v\to v-1)}_{(J\to J-I)}(\nu_T) = \frac{h^2c^2\nu_T^4 S_J^{P,R} A_{(v\to v-1)} B_v}{KT\nu^3_{(v\to v-1)}} \times \exp\left(\frac{-hc(B_v J(J+1)}{KT_R}\right)$$

where $A_{(v\to v-1)}$ is the Einstein coefficient for the spontaneous emission, h the Planck's constant, c the speed of light, $S_J^{P,R}$ the Honl–London factor, $\upsilon_{(v\to v-1)}$ the frequency of the band origin in cm^{-1}, $\upsilon_{(v\to v-1)}$=$E_{(v)} - E_{(v-1))}$ where E_v and $E_{(v-1)}$ are the vibration energies of v and $v-1$ states. This equation can be rearranged for the vibrational transition ($v = 1 \to v = 0$):

$$\ln I_{(J\leftarrow J+1)} = C + \left(-\frac{hcB_1 J(J+1)}{KT_{\mathrm{R}}}\right)$$

$$\text{where } C = \frac{h^2c^2\nu_T^4 S_J^{P,R} A_{(1\to 0)} B_1}{KT\nu^3_{(1\to 0)}}$$

Plotting the relationship between the natural logarithm of the intensity of the rotational lines transition and $J(J+1)$ a straight line was obtained for a Boltzmann's distribution with a slope $\{hcB_1/kT_{\mathrm{R}}\}$.

Fig. 2 shows the transition intensities of the rotational lines of CO molecule resulting from the photodissociation of 0.1 Torr acetone by 193 nm excimer laser with power (4.2 MW/cm^2) at time delay 1 μs between the FT-IR 0.4 cm^{-1} resolution and the laser at different values of J.

Using the Boltzmann's plot the rotational temperature was found to be ($T_{\mathrm{R}} = 2250$ K). The average energy contained in the rotational degrees of freedom can be calculated for the rotational temperature (T_{R}) using the following relation [22]:

$E_{\mathrm{R}} = \frac{3}{2}kT_{\mathrm{R}}$ (for a non-linear polyatomic molecule)

Table 1
The vibrational population distributions for the CO molecule obtained from the photodissociation of 0.1 Torr acetone and 10 Torr He (Exp(I)), 0.2 Torr acetone and 30 Torr He (Exp(II)), and 0.15 Torr acetone (Exp(III)) by the 193 nm excimer laser (4.2 MW/cm^2) at time delay 10 μs

Vibrational population	Exp(I)	Exp(II)	Exp(III)
$P(f_1)$	0.783 ± 0.02	0.78 ± 0.02	0.784 ± 0.02
$P(f_2)$	0.174 ± 0.006	0.175 ± 0.006	0.177 ± 0.006
$P(f_3)$	0.034 ± 0.006	0.037 ± 0.006	0.03 ± 0.006
$P(f_4)$	0.009 ± 0.001	0.008 ± 0.002	0.009 ± 0.001

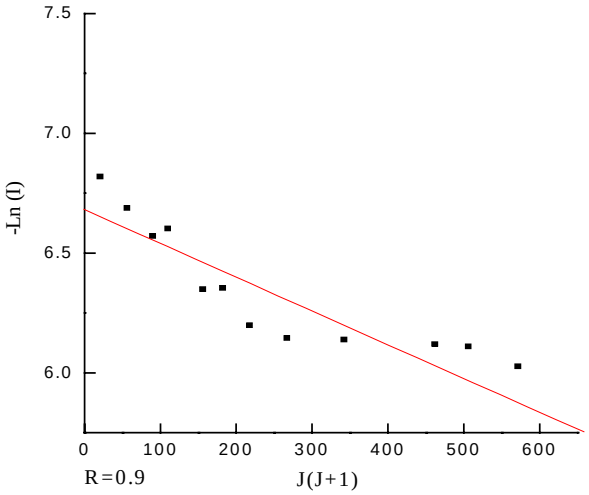

Fig. 2. Shows the relation between the transition intensities of the rotational lines of CO molecule resulting from the photodissociation of 0.1 Torr acetone by 193 nm excimer laser with power 4.2 MW/cm^2 at time delay 1 μs between the FT-IR (0.4 cm^{-1} resolution) and the laser.

$$E_R = kT_R \quad \text{(for a linear polyatomic and diatomic molecule)}$$

The rotational energy of CO molecule was found to be (4.46 kcal/mol).

3.3. Surprisal analysis

For the interpretation of the distribution of energy $P(f_v)$ we need to consider the fact that many different collisions can result in a specific vibrational states. Consequently, we need to find out the fraction of all possible final states for vibrational state (v), we designate this fraction by $P^0(f_v)$, if all states of the products are equally probable (formed with the same rate) then $P(f_v) = P^0(f_v)$. If there is some specific disposal of energy then the rate of populating the states will not be simply proportional to $P^0(f_v)$ and the two distributions will not be identical, so $P^0(f_v)$ serves as a reference against which $P(f_v)$ is compared, because the statistical distribution is the most probable result in the absence of any constraints [23].

The overall deviance from the statistical is measured by the entropy deficiency while the deviance of a particular result (the local deviance) is characterized by the surprisal [24].

Nonstatistical effects can often be represented as a linear surprisal deviation from the information theoritic prior.

Therefore

$$P(f_v) = P^0(f_v) \exp - \lambda_0 - \lambda_v f_v$$

where $P(f_v)$ is the probability of the molecule being in state (v), $P^0(f_v)$ is the statistical vibrational probability for the same state [25], $f_v = (E_v/E_{avl})$ is the fraction of the available energy in state (v), E_v is the vibrational energy in state (v), and E_{avl} is the available energy, λ_v is the vibrational surprisal parameter, and λ_0 the normalization parameter.

Table 2
The surprisal parameters, the surprisal plots intercepts, and the vibrational energies, for the CO molecule obtained from the photodissociation of 0.1 Torr acetone and 10 Torr He (Exp(I)), 0.2 Torr acetone and 30 Torr He (Exp(II)), and 0.15 Torr acetone (Exp(III)) by the 193 nm excimer laser (4.2 MW/cm^2) at time delay 10 μs

Vibration population	Exp(I)	Exp(II)	Exp(III)
λ_v	−11.44	−11.84	−11
λ_0	−1.263	−1.274	−1.246
E_v (kcal/mol)	2.226	2.284	2.189

The photodissociation of the three mixtures of acetone and He gases with pressures I (0.1 Torr acetone and 10 Torr He), II (0.2 Torr acetone and 30 Torr He), or III (0.15 Torr acetone) by 193 nm excimer laser with power (4.2 MW/cm^2) at time delay 10 μs produces vibrationally excited CO molecule. The populations of the four vibrational levels are given in Table 2.

The surprisal plots $-\ln[P(f_v)/P^0(f_v)]$ versus f_v for the three experiments are shown in Fig. 3. A linear surprisal plot with slop λ_v were obtained and the extrapolation to $f_v = 0$ gives an estimate of the dark $v = 0$ population required to normalize the total vibrational energy distributions. Table 2 summarizes the vibrational surprisal parameter λ_v, the normalization parameter λ_0, and the vibrational energies for experiments (I, II, and III).

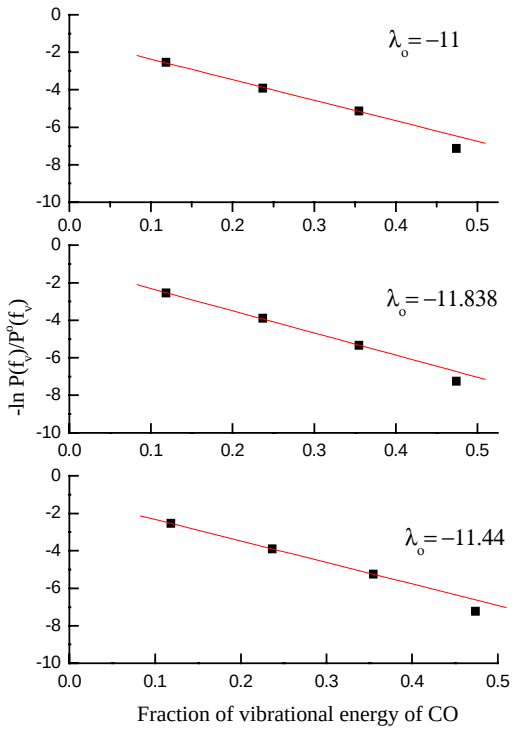

Fig. 3. The surprisal plots for the fraction of the available energy of CO molecule obtained from the photodissociation of 0.1 Torr acetone and 10 Torr He (Exp(I)), 0.2 Torr acetone and 30 Torr He (Exp(II)), from the bottom, and 0.15 Torr acetone (Exp(III)) by the 193 nm excimer laser (4.2 MW/cm^2) at time delay 10 μs.

Table 3
The vibrational population distributions for the vibrational levels of CO molecule (v = 0, 1, 2, 3, 4) obtained from the photodissociation of 0.1 Torr acetone and 10 Torr He (Exp(I)), 0.2 Torr acetone and 30 Torr He (Exp(II)), and 0.15 Torr acetone (Exp(III)) by the 193 nm excimer laser (4.2 MW/cm^2) at time delay 10 μs

Vibration population	Exp(I)	Exp(II)	Exp(III)
$N(v_0)$	0.717	0.712	0.72
$N(v_1)$	0.22	0.224	0.219
$N(v_2)$	0.049	0.05	0.049
$N(v_3)$	0.0095	0.01	0.0084
$N(v_4)$	0.0027	0.0029	0.00246
$T_{vib.}$ (K)	2245 ± 70	2270 ± 75	2200 ± 80

The vibrational population distributions for the first four vibrational levels of CO molecule in addition to the dark population for the photodissociation of the three mixtures by the 193 nm excimer laser (4.2 MW/cm^2) at time delay 10 μs and the vibrational temperature are given in Table 3.

3.4. The vibrational temperature of CO molecule

The intensity of the emitted radiation depends on the population of molecules in the higher vibrational energy levels, following the Boltzmann's distribution:

$$N_v = N_0 \exp - \left(\frac{\Delta E_v}{KT_v}\right)$$

where T_v is the vibrational temperature, ΔE_v is the energy difference between the upper and lower vibrational states:

So the Boltzmann's relation becomes:

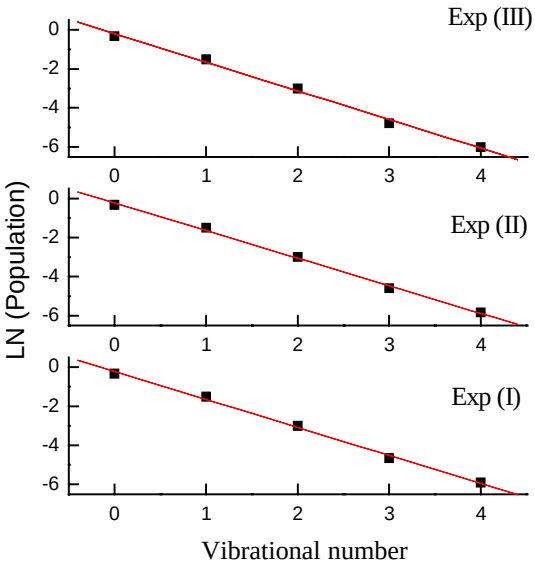

Fig. 4. The Boltzmann's plots for CO bond vibration resulting from the photodissociation of 0.1 Torr acetone and 10 Torr He (Exp(I)), 0.2 Torr acetone and 30 Torr He (Exp(II)), and 0.15 Torr acetone (Exp(III)) by the 193 nm excimer laser at time delay 10 μs from the bottom.

$$\ln N_v = \ln N_0 - \left(\frac{(3212.85)v}{T_v}\right)$$

plotting the relationship between ($\ln N_v$) versus the vibrational number straight lines were obtained for a Boltzmann's population with a slope (3212.85/T_v). This slope can be used to determine the vibrational temperature. The vibrational temperature of CO molecule resulting from the photodissociation of a mixtures from 0.1 Torr acetone and 10 Torr He, 0.2 Torr acetone and 30 Torr He, and 0.15 Torr He gases by 193 nm excimer laser (4.2 MW/cm^2) at time delay 10 μs, were determined here by Boltzmann's plots.

Plotting the relationship between the natural logarithm of the vibrational populations in Table 3 and the vibrational number straight lines were obtained for the three mixtures. The vibrational populations were found to be strongly decreasing with increasing the vibrational number resembling the Boltzmann's distribution as seen in Fig. 4.

4. Theoretical models

4.1. Prior distribution model

The prior distribution model, applied by Hall et al. [25] based on the rigid rotor harmonic oscillator (RRHO) approximation for the photodissociation of a general non linear polyatomic molecules to a linear or a non linear polyatomic molecules [26].

The theoretical approach to the construction the prior function has much in common with the application of statistical theories of the unimolecular dissociation [27,28].

On applying this model on the sequential photolysis of acetone by 193 nm photon, the available energy of the first is (63.4 kcal/mol), this energy undergoes distribution among acetyl and methyl fragments. The average fractions of the available energies in these fragments vibration are given by

$$< \underset{v}{f}\,\mathrm{CH_3CO} >= \frac{\Gamma 22.5}{\Gamma 12\Gamma 10.5}\int_0^1 \underset{v}{f}^{9.5}(1-\underset{v}{f})^{12}\,\mathrm{d}\underset{v}{f} \qquad (1.1)$$

$$< \underset{v}{f}\,\mathrm{CH_3} >= \frac{\Gamma 22.5}{\Gamma 6\Gamma 16.6}\int_0^1 \underset{v}{f}^{6}(1-\underset{v}{f})^{15.5}\,\mathrm{d}\underset{v}{f} \qquad (1.2)$$

where the fraction of the available energy in vibration f_v is the ratio of the average vibrational energy and the available energy. So, the average vibrational energies of acetyl and methyl fragments are (33.8 and 8.45 kcal/mol).

The fraction of the available energies in the internal motions for acetyl and methyl radicals are given by

$$< \underset{I}{f}\,\mathrm{CH_3CO} >= \frac{\Gamma 22.5}{\Gamma 13.5\Gamma 9}\int_0^1 \underset{I}{f}^{13.5}(1-\underset{I}{f})^{8}\,\mathrm{d}\underset{I}{f} \qquad (1.3)$$

$$< \underset{I}{f}\,\mathrm{CH_3} >= \frac{\Gamma 22.5}{\Gamma 7.5\Gamma 15}\int_0^1 \underset{I}{f}^{7.5}(1-\underset{I}{f})^{14}\,\mathrm{d}\underset{I}{f} \qquad (1.4)$$

The average internal energies of acetyl and methyl radicals are (38 and 21.13 kcal/mol). The available energy of the

second step is the difference between the internal energy of the acetyl radical and bond dissociation energy of the second (C–C) bond is (26.54 kcal/mol). The average fraction of the available energies in vibration for the second methyl and CO molecule are given by

$$< \underset{v}{f}\,\mathrm{CH_3} >= (s+4)\int_0^1 \underset{v}{f}\,(1-\underset{v}{f})^4\,\mathrm{d}\underset{v}{f} \tag{1.5}$$

$$< \underset{v}{f}\,\mathrm{CO} >= \frac{1}{11}[(1-\underset{v}{f})^{10}(1+10\underset{v}{f})]|_{f_v}^{f_{v+1}} \tag{1.6}$$

So, vibrational energies of methyl radical and CO fragment are (3.34 and 0.49 kcal/mol). The average fraction of the available energies in rotation for methyl radical and CO fragment are given by

$$< \underset{R}{f}\,\mathrm{CH_3} >= (5)\int_0^1 \underset{R}{f}\,(1-\underset{R}{f})^4\,\mathrm{d}\underset{R}{f} \tag{1.7}$$

$$< \underset{R}{f}\,\mathrm{CO} >= (10)\int_0^1 \underset{R}{f}\,(1-\underset{R}{f})^9\,\mathrm{d}\underset{R}{f} \tag{1.8}$$

The average rotational energies of these fragments are (4.46 and 2.73 kcal/mol).

4.2. The impulsive model

This model proposed firstly by Busch and Wilson [29] for the photodissociation of the triatomic molecule, and applied by Trentelman et al. [22] on the two steps photolysis of acetone by 193 nm photons. In which the two C–C bonds of acetone breaks apart due to the vibrational motion, without general equilibration of the internal energy. These models related the bond breaking to the forces and torques produced between the fragments and use it to describe the translational, vibrational, and rotational excitation in he separating fragments.

The available energy on the fragments after breaking the two bonds is (52.3 kcal/mol). So, the available energy in each impulsive step is given by

$$E_{\mathrm{avl}(1)} = \left(\frac{\mu_{\mathrm{C–C}}}{m_{\mathrm{C}}}\right) E_{\mathrm{avl}} \tag{2.1}$$

This energy undergoes partition among acetyl and methyl fragments according to the masses of the recoiling carbon atoms, so the total energies of acetyl and methyl fragments are:

$$E_{\mathrm{CH_3}} = \left(\frac{\mu_{\mathrm{C–C}}}{m_{\mathrm{C}}}\right) E_{\mathrm{avl}(1)},$$
$$E_{\mathrm{CH_3CO}} = \left(\frac{\mu_{\mathrm{C–C}}}{m_{\mathrm{C}}}\right) E_{\mathrm{avl}(1)} \tag{2.2}$$

These total energies undergoes distribution among the translational, vibrational, and rotational degrees of freedom of them. The translational energies of the acetyl and methyl fragments are given by

$$E_T(\mathrm{CH_3}) = \left(\frac{m_{\mathrm{C}}}{m_{\mathrm{CH_3}}}\right) E_{\mathrm{CH_3}},$$
$$E_T(\mathrm{CH_3CO}) = \left(\frac{m_{\mathrm{C}}}{m_{\mathrm{CH_3}}}\right) E_{\mathrm{CH_3CO}} \tag{2.3}$$

So, the internal energies of the acetyl and methyl fragments are the difference between the total energies and the translational energies of each radical (9.47 and 2.63 kcal/mol). Now the total available energy of the second step is the summation of the internal energy of the acetyl radical and the available energy of the second impulsive step was found to be (35.72 kcal/mol). As in the first impulsive step the total energy of methyl and CO fragments are (17.85 kcal/mol); consequently the translational energies of these fragments and by adding the translational energy of their parent acetyl radical which is distributed among them depending on their masses are given by:

$$E_T{}^{(\mathrm{tot})}(\mathrm{CO}) = E_T(\mathrm{CO}) + \left(\frac{m_{\mathrm{CO}}}{m_{\mathrm{CH_3CO}}}\right) E_T\mathrm{CH_3CO} \tag{2.4}$$

$$E_T{}^{(\mathrm{tot})}(\mathrm{CH_3}) = E_T(\mathrm{CH_3}) + \left(\frac{m_{\mathrm{CH_3}}}{m_{\mathrm{CH_3CO}}}\right) E_T\mathrm{CH_3CO} \tag{2.5}$$

By conservation of the angular momentum, the vibrational and rotational energies of the methyl and CO fragments with (C–C=O) bond angle $\chi = (128^\circ)$ at the moment of dissociation [30] are:

$$E_v(\mathrm{CH_3}) = \left(1-\frac{m_{\mathrm{C}}}{m_{\mathrm{CH_3}}}\right) E\mathrm{CH_3}\cos^2\chi \tag{2.6}$$

$$E_V(\mathrm{CO}) = \left(1-\frac{m_{\mathrm{C}}}{m_{\mathrm{CO}}}\right) E\mathrm{CO}\cos^2\chi \tag{2.7}$$

$$E_R(\mathrm{CH_3}) = \left(1-\frac{m_{\mathrm{C}}}{m_{\mathrm{CH_3}}}\right) E\mathrm{CH_3}\sin^2\chi \tag{2.8}$$

$$E_R(\mathrm{CO}) = \left(1-\frac{m_{\mathrm{C}}}{m_{\mathrm{CO}}}\right) E\mathrm{CO}\sin^2\chi \tag{2.9}$$

4.3. Statistical adiabatic impulsive model

This model reflects both the impulsive model nature of reactions and with large barriers as well as the statistical distribution of energy in addition to the barrier height [31]. The total available energy $E^{(\mathrm{tot.})}$ for the photolysis of acetone by 193 nm photon is (63.4 kcal/mol) divided into two energy reservoirs: one which is statistical $E^{(\mathrm{stat.})}$ and the other is impulsive $E^{(\mathrm{imp.})}$. Where the statistical reservoir, is the energy from the transition state TS up to the total available energy. But the impulsive reservoir, is the energy of the transition state TS relative to the ground state energy of the products. The energy of the transition state acetyl radical has been calculated by Mao et al. to be (18 kcal/mol) [32].

According to this model acetone undergoes photolysis into two steps: the first step is pure impulsive to acetyl and methyl fragments, the acetyl fragment undergoes fragmentation to methyl and CO fragments in such away that the

available energy up the TS distributed according to the prior distribution model, but the energy of the transition state distributed according to the impulsive model.

4.3.1. First step

The available energy of this step is determined from Eq. (2.1) to be (31.7 kcal/mol); this energy distributed among acetyl and methyl fragments, so the total energy of these fragments from Eq. (2.2) is (15.85 kcal/mol). This energy undergoes distribution between translational, and internal degrees of freedom. For acetyl and methyl fragments they are (4.42 and 11.43 kcal/mol) and (12.68 and 3.17 kcal/mol), respectively, as calculated by Eq. (2.3).

4.3.2. Second step

The total available energy of the second is the summation of the internal energy of acetyl fragment and the available energy of the second step after neglecting the bond dissociation energy of the second C–C bond is (31.6 kcal/mol).

The impulsive reservoir: the energy of the transition state acetyl radical (18 kcal/mol) undergoes partition among the translational, vibrational, and rotational degrees of freedom of methyl and CO fragments according to the impulsive model. So, the total translational energies of these fragments are (8.74 and 6.73 kcal/mol)as in Eqs. (2.4) and (2.5). By the same way the vibrational and rotational energies of the methyl and CO fragments are (0.682 and 1.12 kcal/mol) and (1.95 and 3.19 kcal/mol), using Eqs. (2.6)–(2.9).

The statistical reservoir: the available energy for this reservoir is (13.62 kcal/mol), this energy undergoes partition between vibrational, and rotational degrees of freedom of methyl and CO fragments according to the prior distribution model. By using Eqs. (1.5) and (1.6) the vibrational energies of the methyl and CO fragments are (2.27 and 0.0158 kcal/mol).

So, total vibrational energies of methyl and CO fragments from the two reservoirs are (2.95 and 1.97 kcal/mol). Similarly, the total rotational energies of these fragments are (3.39 and 4.43 kcal/mol) using Eqs. (1.7) and (1.8) and from impulsive reservoir.

5. Discussion

The prior distribution model predicts the vibrational energy of the CO fragment to be (0.49 kcal/mol) which is about one fourth the experimentally measured one (2.2 kcal/mol). Similarly, the rotational energy is (2.43 kcal/mol) which is about half the measured value (4.46 kcal/mol). But the impulsive model predicts the vibrational energy of the same fragment to be (3.87 kcal/mol) which is higher than the measured value, While, the rotational energy is (6.34 kcal/mol) is high in comparison with the measured value.

The statistical adiabatic impulsive model as mentioned above is the intermix between both the prior distribution and the impulsive models. According to this model the vibrational energy of CO fragment is about (2 kcal/mol) which nearly equal what is measured experimentally and the rotational energy is (4.43 kcal/mol) is the same as the measured value. Also the translational energy of methyl and CO fragments resulting from the photolysis of acetone by 193 nm photons have been measured by Trentelman et al. [22], consequently for CO fragment to be (6.6 ± 1.2 kcal/mol) nearly equals the predicted value by this model (6.73 kcal/mol). For the primary methyl fragment is (10.5 ± 1.9 kcal/mol) nearly equals the predicted (8.74 kcal/mol), for the secondary methyl radical the value is (12.1 ± 1.9 kcal/mol) which nearly equals the predicted value (12.68 kcal/mol) refer to Table 4.

Table 4
The translational, vibrational, and rotational energies of CO molecule and methyl radicals resulting from the photodissociation of acetone by absorption of 193 nm photon calculated by the prior distribution, impulsive, statistical adiabatic impulsive models, and the experimentally measured values

Fragment	Prior distribution	Impulsive	Statistical adiabatic impulsive	Experimental
Trans. CH_3	–	10.5	12.68	12.1±1.9[a]
Vib. CH_3	8.45	} 2.63	} 3.17	–
Rot. CH_3	12.68			–
Trans. CO	–	10.03	6.73	6.6±1.2[a]
Vib. CO	0.49	3.87	2	2.2
Rot. CO	2.43	6.73	4.43	4.46
Trans. CH_3	–	15.56	8.74	10.5±1.9[a]
Vib. CH_3	3.73	1.35	2.95	–
Rot. CH_3	4.46	2.22	3.39	–

[a] Ref. [22].

Gaines et al. [33] repotted that acetone molecule absorbing 193 nm photon and excited to 3S Rydberg state, where in this state it has little excess energy of vibration 425 cm^{-1}, so, little vibrational redistribution occurs, the 3S Rydberg state is predissociative and crossing the to $\{S_1, T_1\}$ surface is affected via motions of the C(CO)C skeleton. This results were found to support the first impulsive step in the statistical adiabatic impulsive model which depends on the torques and forces (little vibrational energy distribution).

References

[1] J.G. Calvert, J.N. Pitts, Photochemistry, Wiley, New York, 1966.
[2] E.K.C. Lee, R.S. Lewis, Adv. Photochem. 1 (1980) 12.
[3] M. Baba, H. Shinohara, N. Nishi, N. Hirota, Chem. Phys. 83 (1984) 221.
[4] M. Reinsch, M. Klessinger, J. Phys. Org. Chem. 81 (1990) 3.
[5] J. Michl, V. Bonacic-Koutecky, Electronic Aspects of Organic Photochemistry, Wiley, New York, 1990, p. 378.
[6] H. Zuckermann, B. Schmitz, Hass, J. Phys. Chem. 92 (1988) 4835.
[7] M. Brouard, M.T. Mc Pherson, M.J. Pilling, J.M. Tulloch, A.P. Williamson, Chem. Phys. Lett. 113 (1985) 413.
[8] S.W. North, D.A. Blank, Y.T. Lee, J. Chem. Phys. 102 (1995) 4447.

[9] P. Potzinger, G. von Bunan, B. Bunsen, J. Phys. Chem. 72 (1968) 195.
[10] A. Gandini, P.A. Hackett, J. Am. Chem. Soc. 99 (1977) 6195.
[11] D.J. Donaldson, S.R. Leone, J. Phys. Chem. 88 (1986) 817.
[12] E.L. Woodbridge, T.R. Fletcher, S.R. Leone, J. Phys. Chem. 92 (1988) 5387.
[13] A. Buzza, E.M. Snyder, A.W. Castleman, J. Chem. Phys. 104 (1996) 5040.
[14] S.K. Kim, S. Pederson, A.H. Zewail, J. Chem. Phys. 103 (1995) 477.
[15] S.K. Kim, A.H. Zewail, Chem. Phys. Lett. 250 (1996) 279.
[16] J.C. Owrutsky, A.P. Baronavski, J. Chem. Phys. 108 (1998) 6652.
[17] T. Shibata, H. Li, H. Katayangi, T. Suzuki, J. Phys. Chem. 102 (1998) 3643.
[18] Y. Badr, S. Abd elwanees, A.M. Mahmoud, J. Photochem. Photobiol. A Chem., available online.
[19] D. Baurecht, W. Neuhausser, U.P. Fringeli, in: J.A. De Hasech (Ed.), Proceedings of the 11th International AIP Conference on Proceeding, American Institute of Physics, 1998.
[20] T.R. Fletcher, S.R. Leone, J. Chem. Phys. 88 (1988) 4720.
[21] C. Chakerian, R.H. Tipping, J. Mol. Spectrosc. 99 (1983) 431.
[22] K.A. Trentelman, S.H. Kable, D.B. Moss, P.L. Houston, J. Chem. Phys. 91 (1989) 7498.
[23] R.D. Levine, R.B. Bernstein, Acc. Chem. Res. 7 (1974) 393.
[24] R.B. Bernstein, R.D. Levine, Adv. Atom. Mol. Phys. 11 (1975) 215.
[25] G.E. Hall, H.W. Metzler, J.T. Muckerman, J.M. Preses, R.E. Weston, J. Chem. Phys. 102 (1995) 6660.
[26] J.T. Muckerman, J. Phys. Chem. 93 (1989) 179.
[27] R.A. Marcus, J. Chem. Phys. 20 (1952) 359.
[28] G.M. Wieder, R.A. Marcus, J. Chem. Phys. 37 (1962) 1835.
[29] G.E. Busch, K.R. Wilson, J. Chem. Phys. 56 (1972) 3626.
[30] S. Deshmaukh, J.D. Myers, S.S. Xantheas, Hess, J. Phys. Chem. W.P. 98 (1994) 12535.
[31] D.L. Osborn, H. Choi, D.H. Mordaunt, R.H. Bise, D. Neumark, J. Chem. Phys. 106 (1997) 3049.
[32] W. Mao, Q. Li, F. Kong, M.J. Huang, Chem. Phys. Lett. 283 (1998) 114.
[33] G.A. Gaines, D.J. Donaldson, S.J. Strickler, V. Vaida, J. Phys. Chem. 92 (1988) 2762.